Published OnlineFirst July 17, 2018; DOI: 10.1158/2326-6066.CIR-18-0037

Cancer Immunology Miniature

Cancer Immunology Research

Response to Immune Checkpoint Inhibition in Two Patients with Alveolar Soft-Part Sarcoma

Jeremy Lewin[1], Scott Davidson[2,3], Nathaniel D. Anderson[3], Beatrice Y. Lau[4], Jacalyn Kelly[2,5,6], Uri Tabori[2,5,7], Samer Salah[1], Marcus O. Butler[1], Kyaw L. Aung[1], Adam Shlien[2,3], Brendan C. Dickson[4], and Albiruni R. Abdul Razak[1]

Abstract

Alveolar soft-part sarcoma (ASPS) is a morphologically distinctive mesenchymal tumor characterized by a canonical ASPL–TFE3 fusion product. In the metastatic setting, standard cytotoxic chemotherapies are typically ineffective. Studies have suggested modest clinical response to multitargeted receptor tyrosine kinase inhibitors. Here, we report sustained partial responses in two patients with immune checkpoint inhibition treated with either durvalumab (anti–PD-L1) alone or in combination with tremelimumab (anti–CTLA-4), which appeared unrelated to tumor immune infiltrates or mutational burden. Genomic analysis of these patients, and other cases of ASPS, demonstrated molecular mismatch-repair deficiency signatures. These findings suggest that immune checkpoint blockade may be a useful therapeutic strategy for ASPS. *Cancer Immunol Res; 6(9); 1001–7. ©2018 AACR.*

Introduction

Alveolar soft-part sarcoma (ASPS) is a rare mesenchymal tumor that typically arises in adolescent and young adults (1). Tumors usually present as a slow-growing mass but metastatic disease is frequently identified at diagnosis (2). Morphologically, ASPS is characterized by a stereotypic pattern of nested cells separated by fibrous septae, which are often associated with a pseudoalveolar architecture. Molecularly, tumors are characterized by an unbalanced translocation between Xp11 and 17q25, leading to the formation of an ASPSCR1–TFE3 chimeric transcription factor (3). Despite slow tumor growth, the 5-year overall survival is poor at 20% (4, 5).

Given the rarity of ASPS, the literature is limited to small case series. Aside from surgery, there are few therapeutic options, with data suggesting limited value of systemic therapies (6, 7). Antiangiogenic agents have been investigated (8, 9) but the benefits are typically not durable. Given the need for effective therapy, we enrolled 2 patients with ASPS in early-phase trials utilizing mono or combination therapy with durvalumab, a monoclonal antibody (mAb) delivered intravenously that blocks the interaction of programmed death ligand 1 (PD-L1) and PD-1. In parallel, we conducted a multipronged preclinical institutional investigation into ASPS, including the samples from the above 2 patients.

Materials and Methods

Tumors classified as ASPS were identified from an institutional database (identified since 1990) following REB approval. A pathology re-review was conducted by a dedicated sarcoma pathologist (BCD) based on the criteria detailed in the WHO Classification of Tumors of Soft Tissue and Bone.

Immunohistochemistry (IHC)

IHC was performed using standard methods. The Dako Autostainer Link 48 was used for CD3 (clone: F7.2.38; Dako), CD4 (clone: SP35; Roche), CD8 (clone: C8/144B; Dako), CD20 (clone: L26; Dako), MLH1 (clone: ESO5; Novocastra), MSH2 (clone: FE11; Dako), MSH6 (clone: SP93; Cell Marque), and PMS2 (clone: MRQ-28; Cell Marque). The Ventana Benchmark ULTRA was used for PD-1 (clone: NAT105; Roche) and PD-L1 (clone: SP263; Roche).

Scoring of IHC stains

All slides were quantified by a subinvestigator (B.Y. Lau) with 10% selected for independent secondary quantification (BCD). Tumor-infiltrating lymphocytes (TIL) were assessed using a semiquantitative 4-tiered scale: 0 (no lymphocytes); 1 (1–10/HPF); 2 (11–50/HPF); 3 (51–100/HPF); 4 (>100/HPF) (10). In addition, TIL staining with PD-L1 and PD-1 was also scored, whereby the overall percentage of positive cells on the entire slide was quantified. This latter method was also used to assess PD-L1 tumor staining.

[1]Department of Medical Oncology and Hematology, Princess Margaret Cancer Centre, Toronto, Canada. [2]Program in Genetics and Genome Biology, The Hospital for Sick Children, Toronto, Canada. [3]Department of Paediatric Laboratory Medicine, The Hospital for Sick Children, Toronto, Canada. [4]Department of Pathology and Laboratory Medicine, Mount Sinai Hospital, Toronto, Canada. [5]The Arthur and Sonia Labatt Brain Tumour Research Centre, The Hospital for Sick Children, Toronto, Ontario, Canada. [6]Department of Medical Biophysics, Faculty of Medicine, University of Toronto, Toronto, Ontario, Canada. [7]Division of Hematology/Oncology, The Hospital for Sick Children, Toronto, Ontario, Canada.

Note: Supplementary data for this article are available at Cancer Immunology Research Online (http://cancerimmunolres.aacrjournals.org/).

Corresponding Author: Albiruni R. Abdul Razak, Princess Margaret Cancer Centre/Mount Sinai Hospital, 600 University Avenue (Suite 12-23), Toronto, Ontario M5G2M9, Canada. Phone: 647-970-9845, ext. 5371; Fax: 416-586-5165; E-mail: albiruni.razak@uhn.ca

doi: 10.1158/2326-6066.CIR-18-0037

Published OnlineFirst July 17, 2018; DOI: 10.1158/2326-6066.CIR-18-0037

Sequencing

Tumor DNA extracted from paraffin-embedded samples was prepared using Agilent's exome enrichment kit (Sure Select V5). DNA samples were sequenced on an Illumina HiSeq2500 for whole-exome sequencing and an Illumina HiSeq X for whole-genome sequencing. Base calls and intensities from the Illumina HiSeq 2500 were processed into FASTQ files using CASAVA and/or HAS. The paired-end FASTQ files were aligned to UCSC's hg19/GRCh37 with BWA-mem (v.0.7.8). Picard MarkDuplicates (v.1.108) was used to mark PCR duplicates. Aligned reads were realigned for known insertion/deletion events using SRMA and/or GATK. Base quality scores were recalibrated using the Genome Analysis Toolkit (v.2.8.1).

Mutation calls

Somatic mutations were identified using Mutect and filtered against a panel of healthy control samples. The genome sample was filtered against a panel of noncancer genomes. Mutations were further filtered against common SNPs found in dbSNP (v132), the 1000 Genomes Project (February 2012), a 69-sample Complete Genomics data set (11), and the Exome Sequencing Project (v6500).

COSMIC signature analysis

Signature analysis was performed using the DeconstructSigs R package.

Microsatellite instability (MSI) testing

MSI analysis was carried out using the Promega Panel, consisting of five specific microsatellite loci (Bat-25, Bat-26, NR-21, NR-24, and Mono-27). These five loci are PCR-amplified from DNA of patient tumor and nonmalignant tissue using fluorescently labeled primers. The lengths of the amplified fragments were measured by fluorescent capillary electrophoresis, which produces an electrophoretogram with peaks representing each loci. Comparing the loci lengths of patient tumor and nonmalignant tissue using Peak Scanner Software, a length change of 3 base pairs (bp) or more (which presents as a separate peak for heterozygous length changes) in the tumor relative to the nonmalignant tissue is considered a significant change. A length alteration in one of the five loci of 3 bp or more indicates that the tumor has a low level of MSI (MSI-low). Length alterations in two or more of the five loci indicate that the tumor has a high amount of MSI (MSI-high). If a significant length change is not seen in any of the five loci, the tumor is designated as microsatellite stable (MSS). In addition, immunohistochemical assessment for loss of protein expression for MLH1, PMS2, MSH2, and MSH6 was conducted.

Statistical analysis

Interobserver variability was calculated by Cohen kappa analysis. In the event of discordance, a consensus was reached at reevaluation.

Results

Case histories of two patients on immunotherapy

Patient 1 was a 22-year-old female who in 2014 identified a growing lesion on her dorsal left hand. Imaging revealed a destructive lesion in the 4th/5th metacarpals and the presence of multifocal pulmonary metastases. Biopsy demonstrated a neoplasm composed of polygonal cells with a nested architecture. IHC was positive for TFE3, and molecular testing confirmed the presence of the ASPSCR1–TFE3 fusion product, consistent with ASPS. The patient was treated with a multikinase inhibitor against Aurora A, VEGFRs, and FGFRs (April 2014–July 2014) with progression at the primary site. Subsequently, preoperative radiation was delivered followed by palliative ray amputation. Upon pulmonary progression, between December 2014 and May 2015, she was treated sequentially without benefit on trials with an OX40 agonist and then a NOTCH inhibitor. After further progression, the patient was treated within the D4190C00010 trial, which investigates the combination of durvalumab and tremelimumab (NCT02261220). Treatment was started on June 18, 2015. On October 5, 2015, CT images demonstrated 30% reduction in the sum of target lesions as per Response Evaluation Criteria in Solid Tumors (RECIST; Fig. 1). After 4 cycles of combination treatment, the patient was admitted with an immune-related (irAE) grade 4 diarrhea requiring treatment with intravenous methylprednisolone. A colonoscopy demonstrated features of colitis requiring a 4-month prednisolone taper and drug hold from August 2015 until March 2016. Despite being off therapy for 8 months, the patient continued to have ongoing response in her target lesions with tumor reduction of 53% on March 10, 2016. Given the absence of residual irAE, the patient was retreated with durvalumab from March 22, 2016, until May 31, 2016, completing the treatment as per protocol. On the last follow-up in January 2018, continual response was demonstrated with 73% tumor reduction despite being off therapy for >18 months.

Patient 2 was a 41-year-old female who had undergone resection and postoperative radiation of ASPS in 1998. In June 2012, she presented with a solitary brain metastasis treated with surgical resection. Histologic assessment of the tumor was consistent with her previous ASPS. Postoperatively the patient received whole brain irradiation, and restaging scans confirmed the presence of multifocal pulmonary metastases. After a period of surveillance, the patient was enrolled in a clinical trial investigating a multikinase inhibitor against Aurora A, VEGFRs, and FGFRs (March 2014 to August 2014). In September 2014, due to disease progression, she was enrolled in MEDI 4736-1108, which is a study investigating durvalumab in subjects with advanced solid tumors (NCT01693562). The patient received durvalumab from October 1, 2014, and showed reduction of target lesions of 58% (Fig. 2). Treatment continued until October 14, 2015 (12 months), whereupon CT scans confirmed pulmonary and nodal progression. The patient was subsequently enrolled in additional clinical trials without response and unfortunately succumbed to progressive disease in April 2016.

Preclinical investigations

Simultaneously, a multipronged investigation study into this sarcoma subtype was conducted. Pretreatment immunoprofiling of both patients 1 and 2 showed scant immune infiltration with tumoral PD-L1 positivity of 2% and 0%, respectively, and immune cell PD-1 positivity of 0% (Fig. 3). We sequenced the whole exomes of both patients' tumors (>80× coverage). Exomic characterization demonstrated no excess mutational burden, with mutational levels in keeping with other fusion-driven sarcomas (Supplementary Fig. S1). We searched for signatures of somatic mutations, using an established nomenclature (12). We identified signatures associated with defective

Published OnlineFirst July 17, 2018; DOI: 10.1158/2326-6066.CIR-18-0037

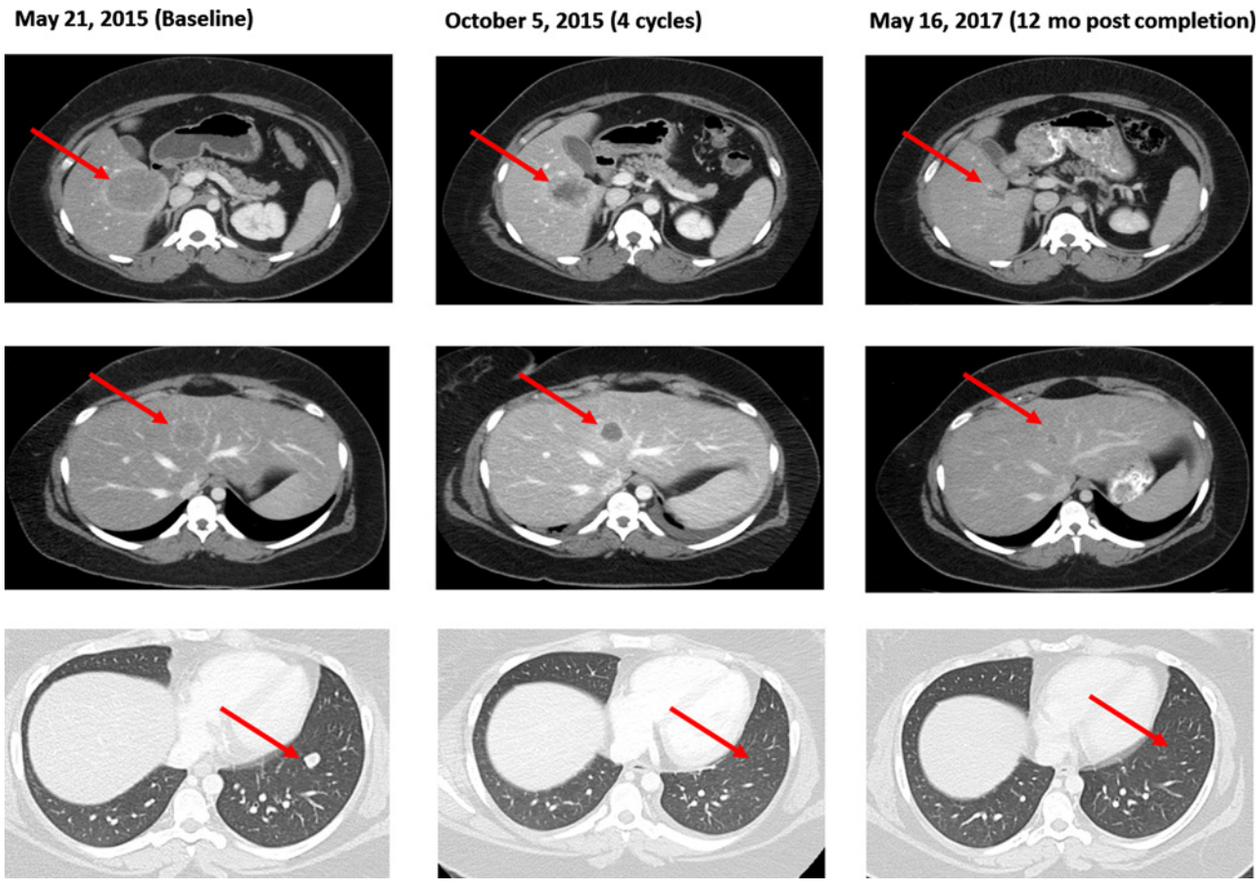

Figure 1.

Axial CT scans showing the response to durvalumab and tremelimumab in patient 1. Baseline CTs conducted on May 21, 2015, show a segment 5 hepatic metastasis (63 mm, top left) segment 4A hepatic metastasis (33 mm, middle left), and left lower lobe pulmonary metastasis (13 mm, lower left). After 4 cycles of combination treatment with durvalumab and tremelimumab (October 5, 2015), the hepatic and pulmonary metastasis showed significant regression with 30% axial tumor volume reduction (middle). Single-agent durvalumab was delivered from March 2016 until May 2016, with ongoing reduction in the patient's target lesions. On the last follow-up on May 16, 2017, the maximum response was achieved showing continued partial response with 73% tumor reduction (right).

mismatch-repair (MMR) pathways in both patients [patient 1: signature (S) 6 (6%), S15 (9%); patient 2: S26 (35%); ref. Fig. 3]. Point mutation and indel analysis did not identify aberrations in the MMR or polymerase genes. IHC for MLH1, MSH2, MSH6, and PMS2 showed intact IHC expression (Supplementary Figs. S2 and S3).

In order to investigate whether the preclinical features were generalizable, we reviewed a total of 18 patients (including the 2 case reports described here) with ASPS (identified since 1990; Supplementary Table S1).

IHC and TILs

Paraffin-embedded tumor was available in 12 cases. PD-1 and PD-L1 expression (threshold set at $\geq$ 1% positive cells) was seen in 17% and 50% of the cases, respectively. $CD3^+$, $CD4^+$, and $CD8^+$ T cell infiltration (threshold set $\geq$ 11 cells/HPF) was seen in 42%, 25%, and 33% of the cases, respectively (Table 1). Clinical responses to PD-1 blockade ($n = 2$) did not appear to correlate with PD-1 or PD-L1 expression or with lymphocyte subtypes. IHC for MLH1, MSH2, MSH6, and PMS2 on patients who underwent exomic characterization (patients 1–7) showed intact IHC expression (Table 1).

Mutational burden quantification

To determine if the sustained response of ASPS patients to immunotherapy could be attributed to a high mutational load, exomic mutation burden was calculated. As expected for tumors lacking a matched–normal control, approximately 60 germline variants per exome were detected. Tumor mutation burden was calculated from all exonic mutations with a variant allele fraction >0.1 called from a minimum coverage of 30× in the tumor. In order to control for the lack of a matched–normal, we performed the same tumor-only analysis on the fusion-driven Ewing sarcoma. We additionally performed the analysis with a matched–normal for Ewing sarcoma and synovial sarcoma (defined by SS18–SSX fusion). In cases where whole-exome sequencing was conducted, no excess mutation burden in ASPS was identified when compared with tumor-only Ewing sarcoma. When analyzed with a matched–normal, both Ewing and synovial sarcoma had low mutation burdens

Published OnlineFirst July 17, 2018; DOI: 10.1158/2326-6066.CIR-18-0037

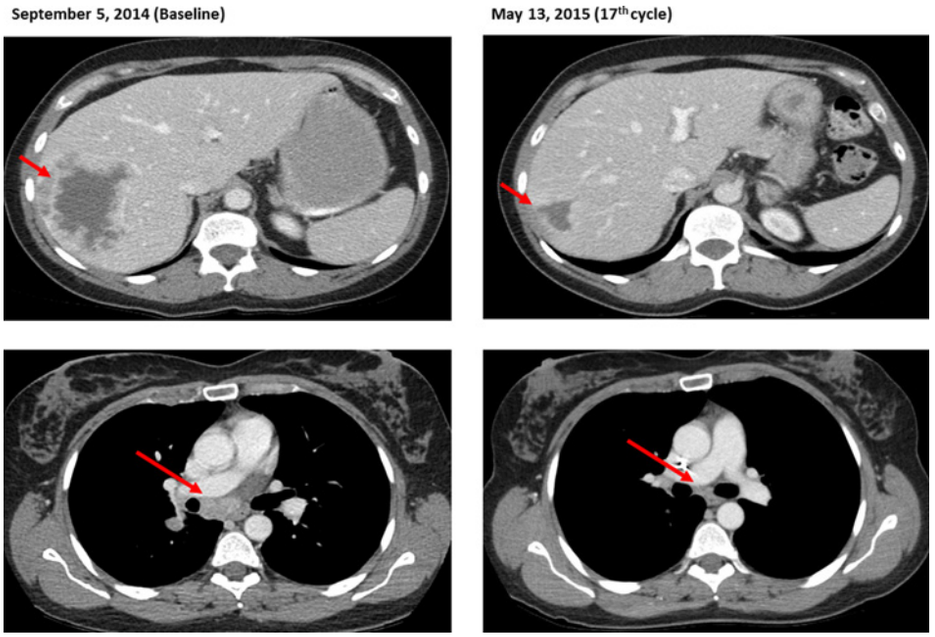

Figure 2.
Axial CT scans showing the response to durvalumab in patient 2. The baseline CTs conducted on September 5, 2014, show a segment 7/8 hepatic metastasis (88 mm, top left), pulmonary metastasis and subcarinal lymph node metastasis (18 mm, bottom left). After 8 months of single-agent durvalumab (May 3, 2015), the maximal tumor reduction of 58% was achieved (middle) with significant reduction in hepatic (25 mm) and subcarinal nodal metastasis (6 mm). Disease progression was documented on October 13, 2015, with increasing pulmonary and hilar nodal disease in association with new pulmonary and nodal disease.

(Supplementary Fig. S1). These data suggest that ASPS mutation burden is similar to other fusion-driven sarcomas.

Mutational signature analysis

Mutational signatures via COSMIC were identified in the MMR deficiency pathway in 5 of 7 cases (patient 1: S6, S15; patient 2: S26; patient 3: S6, S26; patient 4: S6, S26; patient 5: S6, S26), of which 2 of had partial responses to immunotherapy (patients 1 and 2; Fig. 3). The other patients were not treated with immunotherapy. Patient 1 also underwent whole-genome sequencing, which confirmed a COSMIC signature in the MMR deficiency pathway.

Indel analysis

Indel analysis did not confirm aberrations in standard MMR or polymerase genes in patients 1 and 2 (Supplementary Table S2; length values for microsatellite loci). Patient 1's tumor was considered MSS (Supplementary Fig. S4A). Patient 2 would technically have a classification of MSI-L (Supplementary Fig. S4B) from the Promega Panel of five microsatellite sites (13); however, assessing the fluorescence peaks from the MSI electrophoretograms suggested the DNA amplification was suboptimal, with the likely cause being low input DNA concentration.

We developed an informatics pipeline to detect point mutations and indels in single-sample mode using GATK v.3.8 Mutect2 tool and custom, in-house filters. To compensate for the lack of a matched l healthy control, we performed standard point mutation and indel filtering, then filtered against variants common in the population, as well as against a panel of healthy specimens from blood-derived DNA. As a negative control, we performed variant calling and filtering on 145 Ewing sarcoma (also in single-sample mode). On average, the point mutation to indel ratio for ASPS was 5.6:1 ($n = 6$), whereas the point mutation-to-indel ratio for Ewing sarcoma was 10.2 ($n = 145$; Supplementary Fig. S5). In general, Ewing sarcoma tumors had higher ratios; however, most ASPS tumors were within the lower range of Ewing sarcoma tumors, suggesting that ASPS tumors are generally MSS.

With respect to the frameshift frequency, most Ewing sarcoma tumors harbored 10 frameshift mutations/tumor. In contrast, ASPS tumors harbored a wide range of frameshift mutations, including three with frameshift frequencies (5–8 frameshift indels) similar to that seen in Ewing sarcoma range, and three having >30 frameshift indels. Patient 2 had the lowest substitution:indel ratio and a high frequency of frameshift indels. However, patient 1 responded to immunotherapy despite having <10 frameshift indels. Taken together, neither the overall mutation burden nor the ratios of substitutions to indels or frameshift variants provide a genetic explanation for the responses seen.

Discussion

ASPS is a rare sarcoma with limited options in the metastatic setting (8, 9). Both patients 1 and 2 failed to respond to antiangiogenic therapy and after disease progression were placed on either single-agent or combination immune checkpoint inhibitors. Both patients showed substantial and sustained partial responses. Pathologic assessment of IHC and TILs in these patients indicated that the responses to immunotherapy appeared unrelated to baseline numbers of immune cell infiltrates. Exomic characterization demonstrated an MMR deficiency signature, which may, in part, explain these responses; however, conventional MMR aberrations were not identified. Although puzzling, a similar situation has been reported in breast cancer where BRCA mutational deficiency signatures can be identified in patients with no identifiable somatic BRCA mutations (14). The reason for the mutational signature is unclear although was identified in 3 of 5 additional cases where whole-exome sequencing was undertaken. There are several hypotheses to explain why MMR-deficient immune signatures were identified in patients who are MMR proficient with low mutational burden tumors. For example, it is possible that the

Published OnlineFirst July 17, 2018; DOI: 10.1158/2326-6066.CIR-18-0037

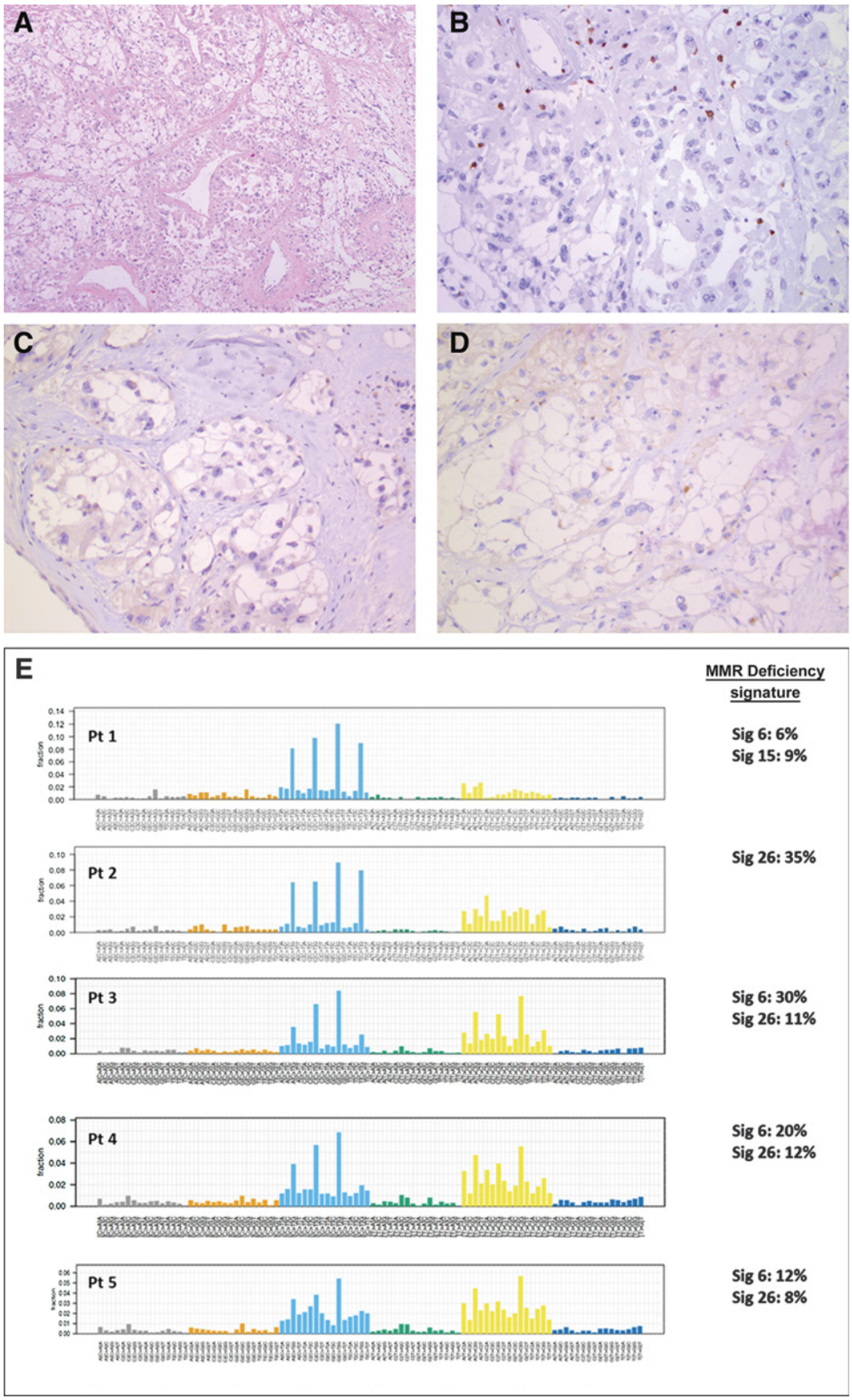

Figure 3.

Histologic, immunohistochemical, and molecular analyses. Morphologic representation of ASPS in patient 1 post neoadjuvant radiation at low magnification showing areas of viable tumor with central loss of cellular cohesion resulting in a pseudoalveolar pattern (**A**, hematoxylin and eosin, 100×). Immunohistochemical analysis of pretreatment resection in patient 1 shows scant T-cell infiltration (**B**, $CD3^+$, 200×) with 0% immune PD-1 positivity and 2% tumoral PD-L1 positivity (**C**, immune $PD\text{-}1^+$, 200×; **D**, tumor $PD\text{-}L1^+$, 200×). Genomic analysis revealed mutational signatures in the MMR deficiency pathway in 5 of 7 cases. The nucleotide context of all substitutions are shown for every patient sequenced. Mutational signatures previously associated with defective MMR are highlighted on the right (**E**).

Published OnlineFirst July 17, 2018; DOI: 10.1158/2326-6066.CIR-18-0037

Table 1. Summary of patient treatment and tumor profiling

						IHC score[a,b]							
Pt	**IO**	**Response**	**WES**	**WGS**	**MMR sig.**	**CD3**	**CD4**	**CD8**	**CD20**	**PD-L1[c]**	**PD-L1[d]**	**PD-1**	**MMR[e]**
1	Yes	PR on D4190C00010 (tremelimumab and durvalumab)	Yes	Yes	Yes	2.3	1.8	1.8	0.0	1.3	0.0	0.3	Intact
2	Yes	PR on MEDI 4736-1108 (durvalumab)	Yes		Yes	2.0	0.3	1.3	0.0	0.0	0.0	0.0	Intact
3			Yes		Yes	3.0	1.8	2.0	0.8	0.0	0.0	1.3	Intact
4			Yes		Yes	1.5	0.8	1.3	0.0	0.0	0.0	0.3	Intact
5			Yes		Yes	2.0	1.0	1.3	0.0	0.5	0.0	0.0	Intact
6			Yes		No	1.0	0.8	1.0	0.0	0.0	0.0	0.0	Intact
7			Yes		No	1.8	0.8	1.0	0.0	0.0	0.0	0.0	Intact
8						1.3	0.0	1.8	0.0	0.0	0.0	0.0	
9						1.3	0.0	1.3	0.0	2.8	0.0	0.0	
10						3.8	0.5	2.5	1.0	0.3	0.0	2.3	
11						1.5	1.5	1.0	N/A	1.0	0.0	0.0	
12						1.0	1.3	1.3	N/A	1.0	0.0	1.0	
Av.						1.63	0.75	1.25	0.23	0.63	0.0	0.33	

Abbreviations: IO, checkpoint inhibitor treatment; PR, partial response; WES, whole-exome sequencing; WGS, whole-genome sequencing; MMR Sig, MMR deficiency signature; N/A, Not available.

[a]Tumor-infiltrating lymphocytes were quantified semiquantitatively using a 4-tiered scale according to Kakavand et al. (10): 0 (no lymphocytes); 1 (1–10/HPF); 2 (11–50/HPF); 3 (51–100/HPF); 4 (>100/HPF).

[b]Interobserver agreement was achieved with a kappa of 0.96.

[c]Score of positive tumor cells/HPF.

[d]Score of positive immune cells/HPF.

[e]MLH1, MSH2, MSH6, and PMS2.

Shaded area denotes no data available

genetic signatures of MMR are caused by noncanonical members of the MMR pathway (rather than the core members that are assayed by IHC). In addition, it is possible that MMR status is not the same across the entirety of the tumor, reflecting genetic heterogeneity in the tumor. Alternatively, nongenetic causes (e.g., exogenous or mutagenic exposures) may contribute.

The low mutational load in ASPS cases appears to contradict the tenet that only highly mutated tumors respond to immune checkpoint inhibition (15). The mechanism of response in ASPS is thus dissimilar to response to immunotherapy in tumors with high rates of mutation in microsatellites, such as those showing biallelic MMR deficiency, which is typically driven by hypermutation profiles (16). The FDA has approved antibodies to PD1 for treatment of non-colorectal MMR-deficient tumors as assessed by either PCR or IHC, based on the study data reporting 53% of those treated had a radiographic responses and 21% had complete responses (17). These clinical data may also be relevant to the translocation-associated variant of renal cell cancer that harbors the ASPL–TFE3 translocation on chromosome Xp11.2 (18).

Although checkpoint inhibitors have revolutionized care for some types of solid tumors, their value for treatment of advanced soft-tissue sarcoma (STS) is uncertain. In the SARC028 trial, pembrolizumab was investigated in selected histologic subtypes of STS (19, 20). In the 40 evaluable patients, the overall response rate was 18%, with responses occurring in subtypes with mutational heterogeneity. Related to ASPS, a few studies report response to checkpoint blockade using immunotherapy (21, 22). Single-agent checkpoint inhibitor studies such as SARC028 did not included ASPS subtypes as it was assumed there would be low efficacy given it is a fusion-driven sarcoma. It remains to be seen whether our findings will be confirmed in immunotherapy studies that include ASPS subsets (NCT02609984, NCT02815995, and NCT02636725).

In STS, it is unknown whether PD-L1 expression may be used as a biomarker (23). Pretreatment tumoral PD-L1 expression was low in both patients 1 and 2; however, this was in keeping with studies where pretreatment PD-L1 expression does not predict response in other tumor types (24). In the biomarker substudy of SARC028, PD-L1 expression was low at baseline and inconsistently associated with clinical response to immunotherapy (20). Similarly, the response to durvalumab in patients 1 and 2 appeared unrelated to baseline immune infiltrate; thus, it is likely that other mechanisms are driving ASPS immunogenicity. For example, TFE3 may modulate the immune response through upregulation of the TGF-B pathway/Foxp3 (25) and activation of CD40 ligand (26).

We acknowledge several limitations in our report. First, this is a small retrospective study of a rare sarcoma subset. Second, there was insufficient sample material to measure elevated MSI at selected tetranucleotide repeats for assessment of MSI. Finally, the lack of matched control subjects made assessment of mutation burden difficult, although this problem was mitigated by cross referencing these samples' genomic information with databases of germline variants. Nevertheless, the observation in these 2 patients, in combination with preclinical work, supports the investigation of immune checkpoint blockade as a therapeutic strategy for ASPS.

Disclosure of Potential Conflicts of Interest

M.O. Butler is a consultant/advisory board member for Merck, Bristol-Myers Squibb, Immunocore, EMD Serono, and Novartis. A.R.A. Razak reports receiving commercial research funding from Medimmune. No potential conflicts of interest were disclosed by the other authors.

Authors' Contributions

Conception and design: J. Lewin, S. Davidson, S. Salah, M.O. Butler, A.R.A. Razak

Development of methodology: J. Lewin, S. Davidson, N.D. Anderson, U. Tabori, M.O. Butler, A. Shlien, A.R.A. Razak

Acquisition of data (provided animals, acquired and managed patients, provided facilities, etc.): J. Lewin, S. Davidson, B.Y. Lau, J. Kelly, S. Salah, M.O. Butler, K.L. Aung, A. Shlien, A.R.A. Razak

Analysis and interpretation of data (e.g., statistical analysis, biostatistics, computational analysis): J. Lewin, S. Davidson, N.D. Anderson, J. Kelly, U. Tabori, M.O. Butler, K.L. Aung, A. Shlien, B.C. Dickson, A.R.A. Razak

Writing, review, and/or revision of the manuscript: J. Lewin, S. Davidson, J. Kelly, U. Tabori, S. Salah, M.O. Butler, K.L. Aung, A. Shlien, B.C. Dickson, A.R.A. Razak

Published OnlineFirst July 17, 2018; DOI: 10.1158/2326-6066.CIR-18-0037

Administrative, technical, or material support (i.e., reporting or organizing data, constructing databases): J. Lewin, S. Davidson, A.R.A. Razak
Study supervision: A.R.A. Razak

Acknowledgments

We acknowledge the support of MedImmune (Gaithersburg, MD) in allowing the publication of these two patients on NCT02261220 and NCT01693562. The authors declare that no funding was received from MedImmune for development or research associated with this manuscript. Funding for this work was directly received from the philanthropic efforts of the Sarcoma Cancer Foundation of Canada and The Princess Margaret Cancer Foundation/Nicol Family Foundation.

Received January 25, 2018; revised April 26, 2018; accepted July 12, 2018; published first July 17, 2018.

References

1. Brennan MF, Antonescu CR, Alektiar KM, Maki RG. Alveolar soft part sarcoma. Management of soft tissue sarcoma. New York, NY: Springer; 2016, pp. 283–9.
2. Postovsky S, Ash S, Ramu I, Yaniv Y, Zaizov R, Futerman B, et al. Central nervous system involvement in children with sarcoma. Oncology 2003;65: 118–24.
3. Ladanyi M, Lui MY, Antonescu CR, Krause-Boehm A, Meindl A, Argani P, et al. The der (17) t (X; 17)(p11; q25) of human alveolar soft part sarcoma fuses the TFE3 transcription factor gene to ASPL, a novel gene at 17q25. Oncogene 2001;20:48–57.
4. Lieberman PH, Brennan MF, Kimmel M, Erlandson R, Garin-Chesa P, Fiehinger B. Alveolar soft-part sarcoma. Cancer 1989;63:13.
5. Portera CA Jr, Ho V, Patel SR, Hunt KK, Feig BW, Respondek PM, et al. Alveolar soft part sarcoma. Cancer 2001;91:585–91.
6. Reichardt P, Lindner T, Pink D, Thuss-Patience P, Kretzschmar A, Dörken B. Chemotherapy in alveolar soft part sarcomas: what do we know? Eur J Cancer 2003;39:1511–6.
7. Roozendaal K, De Valk B, Ten Velden J, Van Der Woude H, Kroon B. Alveolar soft-part sarcoma responding to interferon alpha-2b. Br J Cancer 2003;89:243.
8. Judson I, Scurr M, Gardner K, Barquin E, Marotti M, Collins B, et al. Phase II study of cediranib in patients with advanced gastrointestinal stromal tumors or soft-tissue sarcoma. Clin Cancer Res 2014;20:3603–12.
9. Stacchiotti S, Negri T, Zaffaroni N, Palassini E, Morosi C, Brich S, et al. Sunitinib in advanced alveolar soft part sarcoma: evidence of a direct antitumor effect. Ann Oncol 2011;22:1682–90.
10. Kakavand H, Wilmott JS, Menzies AM, Vilain R, Haydu LE, Yearley JH, et al. PD-L1 expression and tumor-infiltrating lymphocytes define different subsets of MAPK inhibitor–treated melanoma patients. Clin Cancer Res 2015;21:3140–8.
11. Drmanac R, Sparks AB, Callow MJ, Halpern AL, Burns NL, Kermani BG, et al. Human genome sequencing using unchained base reads on self-assembling DNA nanoarrays. Science 2010;327:78–81.
12. Alexandrov LB, Nik-Zainal S, Wedge DC, Aparicio SA, Behjati S, Biankin AV, et al. Signatures of mutational processes in human cancer. Nature 2013;500:415–21.
13. Bacher JW, Flanagan LA, Smalley RL, Nassif NA, Burgart LJ, Halberg RB, et al. Development of a fluorescent multiplex assay for detection of MSI-High tumors. Dis Markers 2004;20:237–50.
14. Davies HR, Glodzik D, Morganella S, Yates LR, Staaf J, Zou X, et al. HRDetect is a predictor of BRCA1 and BRCA2 deficiency based on mutational signatures. Nat Med 2017;23:517–25.
15. Champiat S, Ferté C, Lebel-Binay S, Eggermont A, Soria JC. Exomics and immunogenics: Bridging mutational load and immune checkpoints efficacy. Oncoimmunology 2014;3:e27817.
16. Bouffet E, Larouche V, Campbell BB, Merico D, de Borja R, Aronson M, et al. Immune checkpoint inhibition for hypermutant glioblastoma multiforme resulting from germline biallelic mismatch repair deficiency. J Clin Oncol 2016;34:2206–11.
17. Le DT, Durham JN, Smith KN, Wang H, Bartlett BR, Aulakh LK, et al. Mismatch-repair deficiency predicts response of solid tumors to PD-1 blockade. Science 2017;357:409–13.
18. Argani P, Antonescu CR, Illei PB, Lui MY, Timmons CF, Newbury R, et al. Primary renal neoplasms with the ASPL-TFE3 gene fusion of alveolar soft part sarcoma: a distinctive tumor entity previously included among renal cell carcinomas of children and adolescents. Am J Pathol 2001;159:179–92.
19. Tawbi HA-H, Burgess MA, Bolejack V, Van Tine BA, Schuetze SM, Hu J, et al. Pembrolizumab in advanced soft-tissue sarcoma and bone sarcoma (SARC028): a multicentre, two-cohort, single-arm, open-label, phase 2 trial. Lancet Oncol 2017;18:1493–501.
20. Burgess MA, Bolejack V, Van Tine BA, Schuetze S, Hu J, D'Angelo SP, et al. Multicenter phase II study of pembrolizumab (P) in advanced soft tissue (STS) and bone sarcomas (BS): Final results of SARC028 and biomarker analyses. J Clin Oncol 2017;35:11008.
21. Conley AP, Trinh VA, Zobniw CM, Posey K, Martinez JD, Arrieta OG, et al. Positive tumor response to combined checkpoint inhibitors in a patient with refractory alveolar soft part sarcoma: a case report. J Glob Oncol 2017:009993.
22. Groisberg R, Hong DS, Behrang A, Hess K, Janku F, Piha-Paul S, et al. Characteristics and outcomes of patients with advanced sarcoma enrolled in early phase immunotherapy trials. J Immunother Cancer 2017;5:100.
23. Kim JR, Moon YJ, Kwon KS, Bae JS, Wagle S, Kim KM, et al. Tumor infiltrating PD1-positive lymphocytes and the expression of PD-L1 predict poor prognosis of soft tissue sarcomas. PLoS One 2013;8:e82870.
24. Callahan MK, Postow MA, Wolchok JD. CTLA-4 and PD-1 pathway blockade: combinations in the clinic. Front Oncol 2014;4:385.
25. Lazar AJ, Das P, Tuvin D, Korchin B, Zhu Q, Jin Z, et al. Angiogenesis-promoting gene patterns in alveolar soft part sarcoma. Clin Ca Res 2007;13:7314–21.
26. Huan C, Kelly ML, Steele R, Shapira I, Gottesman SR, Roman CA. Transcription factors TFE3 and TFEB are critical for CD40 ligand expression and thymus-dependent humoral immunity. Nat Immunol 2006;7:1082–91.

Published OnlineFirst July 17, 2018; DOI: 10.1158/2326-6066.CIR-18-0037

Cancer Immunology Research

Response to Immune Checkpoint Inhibition in Two Patients with Alveolar Soft-Part Sarcoma

Jeremy Lewin, Scott Davidson, Nathaniel D. Anderson, et al.

Cancer Immunol Res 2018;6:1001-1007. Published OnlineFirst July 17, 2018.